

A DC-DC converter for electric vehicle application

Thirumalaisamy Bogaraj* , Paul Sweety Jose , Angappan Natarajan ,
Subramanian Karthikeyan 

Department of Electrical and Electronics Engineering, PSG College of Technology, Coimbatore, India.

*Corresponding author: tbr.eee@psgtech.ac.in

Original Research

Abstract:

Received:
7 May 2024
Revised:
3 June 2024
Accepted:
10 June 2024
Published online:
15 December 2024

An innovative Synchronous Buck Converter (SBC) with a wide input voltage range is presented in this article for use in Electric Vehicle (EV) applications. The disadvantages of higher losses in an Asynchronous Buck Converter (ABC) are intended to be addressed by the Synchronous Buck Converter. Fewer losses occur in the circuit when MOSFET (or any controlled switch) is used in place of diode. To enhance system performance, a control approach known as Emulated Peak Current Mode (EPCM) is employed. The design of a broad range input SBC and the investigation of power loss calculations using different control techniques, which are implemented using PSIM, are the primary contributions made in this paper. The buck converter employed in this paper has an output voltage of 12 V and a wider input voltage range of 40 – 75 V. It is utilized by electric vehicles' light and horn systems. Using PSIM software, the SBC using the EPCM, Current Mode Control (CMC), and Voltage Mode Control (VMC) techniques is simulated. Hardware results coincide with the simulation results and thus the results are validated.

© The Author(s) 2024

Keywords: Electric vehicle; Emulated peak current mode; Drain to source resistance; DC-DC converter; Current mode control; Voltage mode control

1. Introduction

Internal Combustion Engine (ICE) vehicles cause air pollution, global warming, and resource depletion. Electric cars, hybrid vehicles, and fuel-cell electric vehicles can overcome the problems of conventional automobiles and provide a solution to these issues [1]. An Electric Vehicle (EV) is powered by an electric motor instead of a conventional diesel or petrol engine. This electric motor is powered by rechargeable batteries that is charged by using electricity. The energy is transmitted to the vehicle by wireless energy transmission such as inductive charging or direct electrical cable connection. Using a battery, flywheel, super capacitor or fuel cell, the electricity can then be stored in, on board vehicle. The Electric Vehicle power supply configurations show that at least one DC-DC converter is required to interface to the DC-link with the Fuel Cell, Battery or Super capacitors module. A DC to DC converter is a category of power converters in electrical engineering and it is an electrical circuit that converts a source of Direct Current from one voltage level to another by storing the input energy. Storage can be either in the form of magnetic field

storage components (inductors, transformers) or in the form of electrical field storage components (capacitors). It is possible to control the amount of power flow between input and output by adjusting the duty cycle. In electrical powertrains, DC-DC converters are being utilized to interface various electrical and electronic circuits. A DC-DC converter is a crucial part of electric cars since they contain several electrical circuits that operate at various voltage levels. It is the key component of electric cars, which are powered by batteries with a high DC voltage. Since EV components can work at high or low voltage levels, DC-DC converters are needed to maintain the voltage value for these components. In electrical cars and other electronic projects that work at various DC levels, DC-DC converters have become an essential component. The DC-DC converter must meet the following requirements like higher efficiency, small size and weight, less ripple in output, regulated power flow and provide regulated output voltage irrespective of the input. This is usually done for controlling output voltage, input current, output current, or for maintaining constant power. Transformer-based converters can provide input-output isolation. Non isolated DC-DC converters are designed to

transfer power from input to output in just one direction [2]. In this paper a Synchronous non isolated DC-DC Converter is designed to supply horn and light system of an Electric Vehicle. Buck converter steps down the voltage from higher voltage to lower voltage.

An efficiency-enhanced Asynchronous Buck Converter (ABC) with threshold compensated freewheeling diode is proposed in [3]. Improvement of the Synchronous Buck Converter (SBC) Dynamic Performance applied to Hybrid Electric Vehicle Regenerative Power Systems is proposed in [4]. A High Capacity SBC for Highly Efficient and Lightweight Charger of Electric Easy Bikes is proposed in [5]. The various control methods of the DC-DC converter are implemented to maintain constant output voltage. Voltage Mode Control (VMC), Current Mode Control (CMC) and Sliding Mode Control (SMC) schemes are designed to maintain load voltage for different load conditions and different supply conditions [6–9].

2. Operating principle

The overall block diagram of Battery-Operated Electric Vehicle is given in Fig. 1.

Buck Converter (BC) is a type of DC-DC converter used to obtain lower output voltage levels from higher input voltage levels. To maximize performance and meet customer requirements, the power converter design must be optimized. Efficiency of the power converter is critical as the industry transitions to higher performance platforms. In [3] an integrated synchronous buck converter was proposed which produces independent multiple outputs with increased efficiency. A lesser regulated voltage than the input voltage is converted by the synchronous buck converter. This converter can supply higher currents and at the same time losses can be minimized. The circuit for conventional and proposed synchronous buck converter is given in Fig. 2a and b.. The SBC consists of two power MOSFET switches, output capacitor, and an inductor. One of the MOSFET act as Upper Side (US) MOSFET and other act as Lower Side (LS) MOSFET. The SBC topology is derived from the control technique of the two MOSFETs involved in the on/off

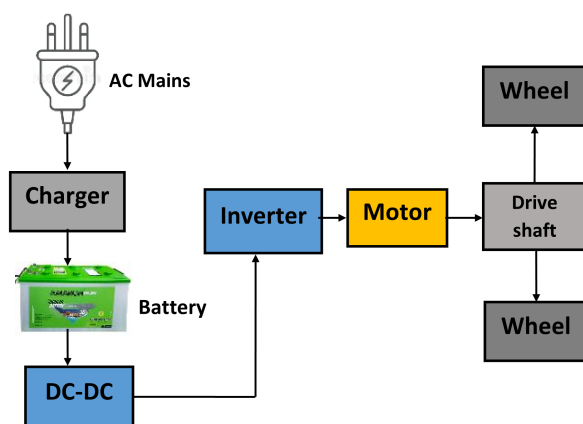


Figure 1. Schematic of Battery-Operated Electric Vehicle.

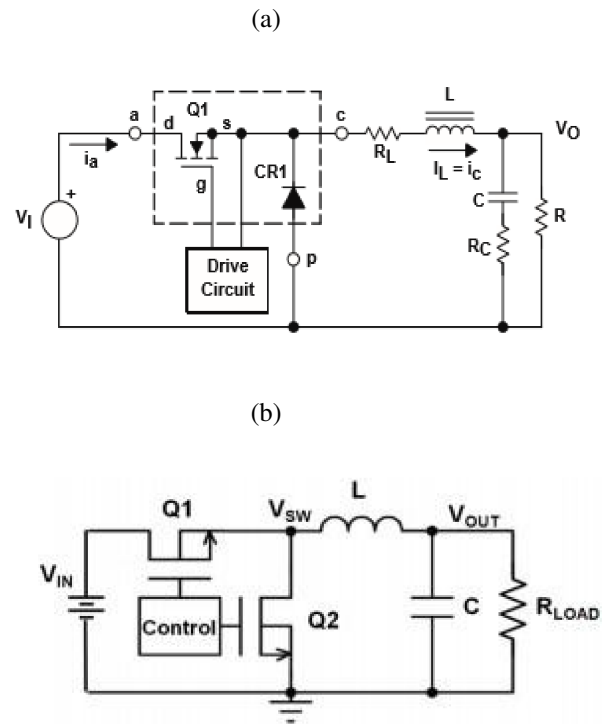


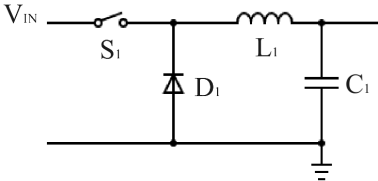
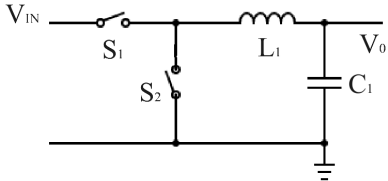
Figure 2. Conventional Buck converter (a) and Schematic of proposed SBC in open loop (b).

switching operation. This synchronized switching operation of MOSFET provides desired the regulated output voltage when the wide range of input is given to the converter. The simultaneous on/off of the MOSFET in synchronous converter is prevented. Bidirectional converters are employed so as to manage the power flow among the source and the load [4]. When Q1 is turned on in Fig. 2b, the MOSFET in upper side is directly connected to the circuit's input voltage side. When Q1 (US-MOSFET) is turned on, load current is provided through the US-MOSFET. If the Q2 (LS-MOSFET) is turned off, the inductor current raises, and energy stored in output capacitor [10].

When Q1 is turned off and Q2 is turned on, current is provided to the load via the LS-MOSFET. The inductor current diminishes during this period, and discharges the LC filter. When both MOSFETs are turned off, LS-MOSFET serves an extra purpose. The LS-MOSFET clamps the switch node voltage through the body of the diode to prevent V_{SW} from going too far negative when the high side MOSFET initially shuts off. Fig. 3 depicts the SBC's continuous conduction mode.

The LC output stage smoothen the switch node voltage to provide a controlled DC output voltage. The MOSFETs are regulated simultaneously to avoid shoot through faults. Shoot through faults happens when both the upper and lower side MOSFETs are turned on together, resulting in dead short circuit to ground. The following Table 1 compares the conventional ABC and the proposed SBC.

Table 1. Comparison of ABC and SBC.

Asynchronous Buck Converter	Proposed Synchronous Buck Converter
	
Fig. 2a Asynchronous Buck Converter	Fig. 2b Synchronous Buck Converter
It consists of one controlled switch	It consists of two controlled switches.
The current flow to the diode is controlled by on-off action of the high side switch.	The on/off action is controlled by low side and high side switch.
Has low efficiency than Synchronous converter	Achieves higher efficiency than Asynchronous converter.
The reason for less efficiency is due to diode in the circuit.	High efficiency is due to low side switch.
Power dissipation across the diode in asynchronous buck converter is given by $P = V_D * I_{out} * (1 - \frac{V_{out}}{V_{in}})$	Power dissipation across MOSFET is given by $P = R_{ON} * I_{out}^2 * (1 - \frac{V_{out}}{V_{in}})$
Diode loss is attributable to the forward voltage V_F . The V_F of the diode increases as a function of current.	Here controlled switch used is MOSFET. On-resistance of MOSFET is less.
Even in the case of a Schottky diode, known for a low V_F value, the level of V_F at 1 A reaches 0.3 to 0.5 V.	The on-resistance of the N channel MOSFET, for example, is extremely low at 50 mΩ.

3. Control technique

The control technique involved in this designed synchronous buck converter is EPCM control. An Emulated Peak Current Mode control method is developed by using a gate sample and hold of the valley current. This gate sampling

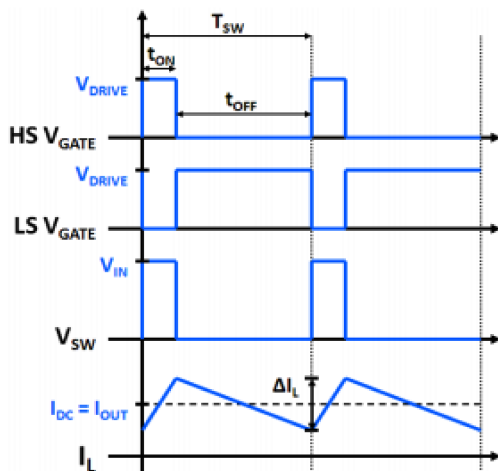


Figure 3. Synchronous buck converter waveforms.

technique removes the slope, compensating ramp's duty cycle dependence and stabilizes the modulator gain over line voltage changes [11].

Emulated Peak Current Mode (EPCM) SBC is shown in the Fig. 4. In the Fig. 4, R_s denotes the gating resistor, V_{in} is the input voltage, V_{sw} is the voltage across the switch, V_R is the reference voltage. Discrete-time models were developed to demonstrate that the required slope of the current, which was simulated but differed from the slope of the actual current, had to change with controller gain in order

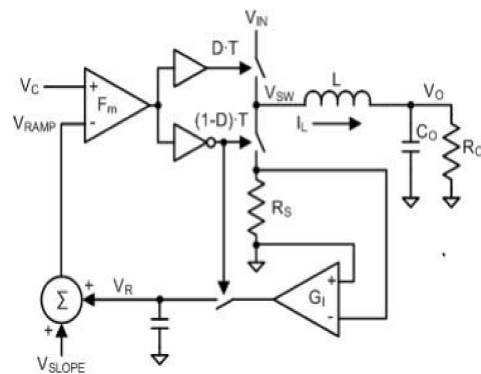


Figure 4. Emulated peak current mode buck converter.

to reduce the computing work needed for slope estimation [12]. Under typical load circumstances, inductor current is always positive and flows from the inductor's input to the output side. Current is made up of a DC as well as an AC component known as the ripple current. For the entire switching period the addition of DC and AC components of the inductor current remains positive, and the converter is said to be operating in Continuous Conduction Mode (CCM) [5].

Modern controllers comprise a circuit that prevents loss of DCM conduction by emulating a diode's current blocking behavior by the use of low-side synchronous MOSFET. This smart diode action is known as the Diode Emulation Mode (DEM), and it serves to switch off the synchronous MOSFET when the circuit detects that the inductor's current is starting to flow in the wrong direction. This circuit monitors the low-side synchronous MOSFET voltage across the R_s and switches OFF the MOSFET when adverse conditions arise.

4. Design specifications

4.1 Power circuit

For the given specifications of the SBC in Table 2, the inductor, capacitor and the other required parameters are calculated

Duty cycle for minimum input voltage ($V_{in\ min}$) = 40 V is

$$D = \frac{V_{out}}{V_{in\ min}} = \frac{12}{40} = 0.3 \quad (1)$$

Duty cycle for maximum input voltage ($V_{in\ max}$) = 75 V is

$$D = \frac{V_{out}}{V_{in\ max}} = \frac{12}{75} = 0.16 \quad (2)$$

Inductance is calculated [9, 13] by taking 40% of I_{pp} is

$$L = \frac{V_{out}}{I_{pp} \times F_{sw}} \times \left(1 - \frac{V_{out}}{V_{in\ max}}\right) \quad (3)$$

$$L = \frac{12}{0.4 \times 8 \times 50 \times 1000} \times \left(1 - \frac{12}{75}\right) = 63 \mu\text{H}$$

Ripple current of inductor is calculated for $V_{in\ min}$ and $V_{in\ max}$.

Table 2. Parameters of synchronous buck converter.

Parameters	Range
Input Voltage ($V_{in\ min}$)	40 V
Input Voltage ($V_{in\ max}$)	75 V
Output voltage (V_{out})	12 V
Output current (I_o)	8 A
Switching frequency (F_{sw})	50 kHz
Ripple voltage	50 mV

For $V_{in\ min} = 40$ V, the Inductor ripple current is found as

$$\Delta I_{L\ min} = \frac{V_{out} \times (V_{in\ min} - V_{out})}{L \times F_{sw} \times V_{in\ min}} = \frac{12 \times (40 - 12)}{63 \times 10^{-6} \times 50 \times 10^3 \times 40} = 2.71 \text{ A} \quad (4)$$

For $V_{in\ max} = 75$ V, the Inductor ripple current is given by

$$\Delta I_{L\ max} = \frac{V_{out} \times (V_{in\ max} - V_{out})}{L \times F_{sw} \times V_{in\ max}} = \frac{12 \times (75 - 12)}{63 \times 10^{-6} \times 50 \times 10^3 \times 75} = 3.25 \text{ A} \quad (5)$$

The output capacitor value for the minimum inductor ripple current is calculated as

$$C_{out\ min} = \frac{\Delta I_{L\ min}}{8 \times F_{sw} \times \Delta V_{out}} = \frac{2.7}{8 \times 50 \times 10^3 \times 40 \times 50 \times 10^{-3}} = 135 \mu\text{F} \quad (6)$$

The output capacitor value for the maximum inductor ripple current is calculated as

$$C_{out\ min} = \frac{\Delta I_{L\ max}}{8 \times F_{sw} \times \Delta V_{out}} = \frac{3.25}{8 \times 50 \times 10^3 \times 40 \times 50 \times 10^{-3}} = 162 \mu\text{F} \quad (7)$$

4.2 Compensator circuit

Due to changes in load and fluctuating input voltage, an open loop DC-DC converter is unable to adjust its output voltage [14] A voltage-mode hybrid resonant buck converter that operates in CCM is chosen and designed. To alleviate this issue, a compensator is utilized, resulting in a steady voltage output from the converter. Compensators are the specialized filters used in the buck converter to obtain the desired constant output voltage [6]. Deep analysis of different types of compensators (type I, type II, type III) were made and implementation of type III compensator for voltage mode control of converter was done [7]. To obtain desired performance type II compensators are used in the converter [8].

The preferred loop crossover frequency is typically placed at the geometric mean of the zero and pole when designing this type of compensator, which is utilized by designers to offer a phase boost to manage the loop [15]. Fig. 5 shows

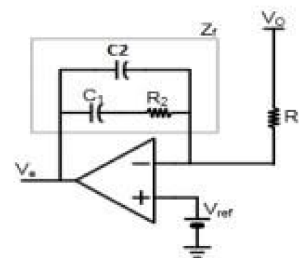


Figure 5. Type II compensator using op-amp.

type II compensator by using op-amp. $G(S)$ is the gain of the op-amp with compensator.

$$G(s) = \frac{V_c(s)}{V_o(s)} = -\frac{Z_f}{Z_i} = -\frac{\left(R_2 + \frac{1}{sC_1}\right)\frac{1}{sC_2}}{\left(R_2 + \frac{1}{sC_1}\frac{1}{sC_2}\right)R_1} \quad (8)$$

Rearranging C_1 and C_2 in the Eqn. (8)

$$G(s) = \frac{V_c(s)}{V_o(s)} = -\frac{s + \frac{1}{R_2C_1}}{sR_1C_2\left(s + \frac{1}{R_2C_2}\right)} \quad (9)$$

Eqn. (9) denotes the gain of the op-amp with compensator.

5. Simulation of the designed SBC

5.1 Emulated peak current mode (EPCM)

Wide range input of SBC with EPCM control technique is simulated using PSIM. The simulated converter provides stable output voltage of 12 V when the wide range of input from 40 V to 75 V is given as input to the converter. In SBC the MOSFET is replaced in the place of diode. The two MOSFETs operate in a synchronous manner so that the both of the MOSFET do not turn ON at the same time. Fig. 6 shows the simulation of synchronous buck converter by using EPCM in PSIM. In EPCM control two loops are involved one is from the output voltage and the other is from the gate resistance of MOSFET.

The output voltage and reference voltage are compared using error amplifier with compensator then the error signal is compared with the current sensed by gate resistor. Then the output is given to SR flip flop so that two MOSFETs are prevented from turning ON at the same time.

The synchronous buck converter circuit is simulated in

PSIM and the outputs were obtained. Fig. 7 a to Fig. 7 h shows the waveform of constant output voltage of 12 V for the variable input voltage and the gate signal of the two MOSFETs. From the complementary waveforms of the gate signals, it is observed that when MOSFET Q1 is in ON condition then the other MOSFET Q2 is in OFF condition. This helps in the synchronous operation of the converter to obtain the stable output voltage.

5.2 Current mode control (CMC)

The simulation circuit of the synchronous buck converter by using current mode control is shown in Fig. 8. The output voltage plots for the input voltages 40 V and 70 V are presented in Fig. 9. Fig. 9 (a) and Fig. 9 (b) shows the input voltage waveform of 40 V and output voltage waveform of 12 V for the 40 V input. Fig. 9 (c) and Fig. 9 (d) shows the input and output voltage waveforms for 70 V input respectively. Gate signal for MOSFETs Q1 and Q2 of SBC are presented in Fig. 9 (e) and Fig. 9 (f) respectively.

5.3 Voltage mode control (VMC)

Simulation of synchronous buck converter is similar to that of Asynchronous buck converter, except that the replacement of MOSFET in the place of diode. The voltage mode control of synchronous buck converter is shown in Fig. 10. Fig. 11 (a) and Fig. 11 (b) illustrates waveforms of the SBC input and output voltages for 40 V input. Fig. 11 (c) and Fig. 11 (d) shows the waveform of the SBC for 65 V and the output voltage of 12 V for the 65 V input. Fig. 11 (e) and 11 (f) shows input put voltage waveform of the synchronous buck converter for 75 V and the output voltage waveform of 12 V for 75 V input. Fig. 11 (g) and Fig. 11 (h) shows the gate signal for the MOSFET Q1 and Q2.

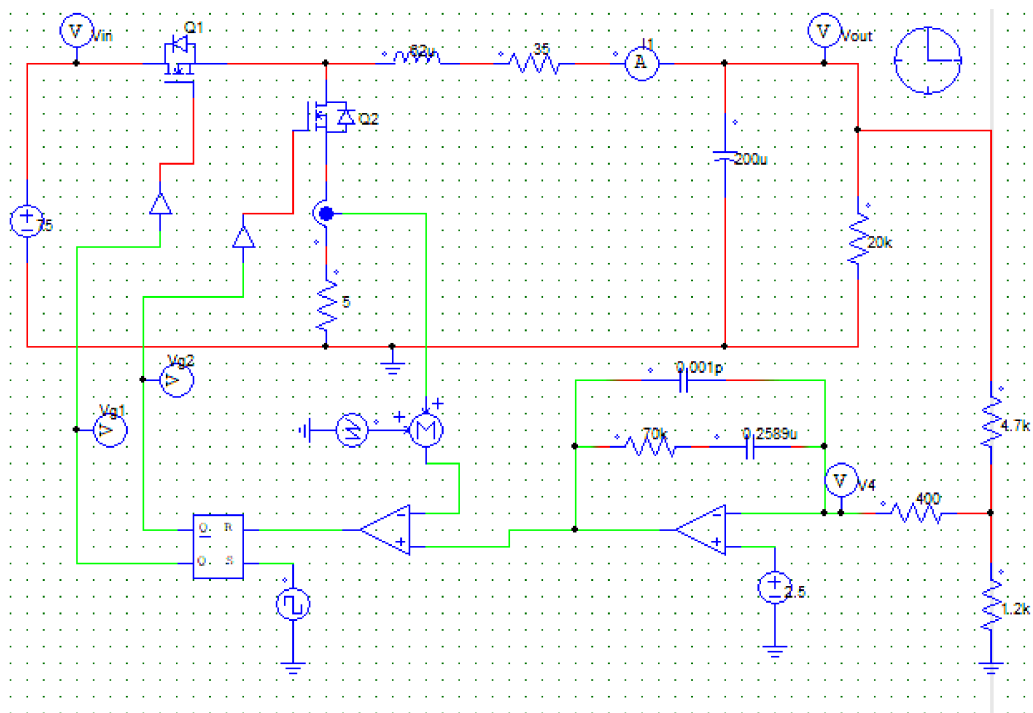


Figure 6. PSIM Simulation of SBC by using EPCM control.

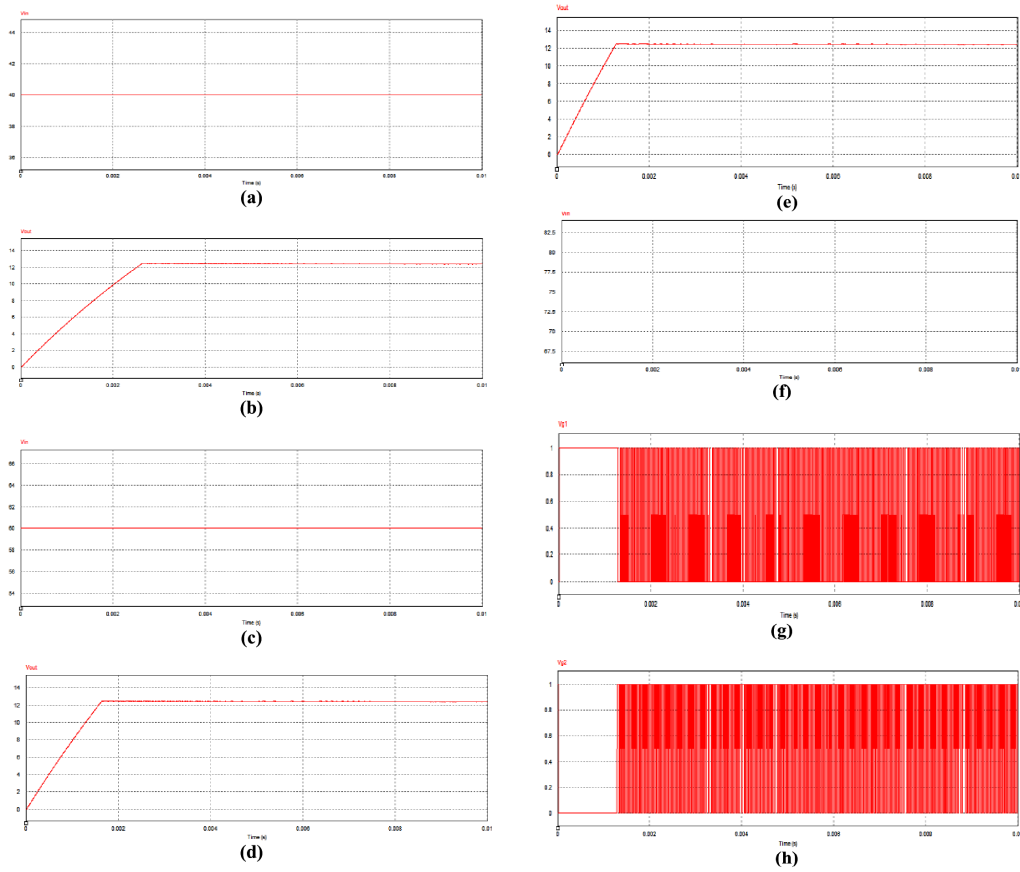


Figure 7. (a) Input voltage of 40 V. (b) Output voltage of 12 V for 40 V input. (c) Input voltage of 60 V. (d) Output voltage of 12 V for 60 V input. (e) Input voltage of 75 V. (f) Output voltage of 12 V for 75 V input. (g) Gate signal for MOSFET Q1. (h) Gate signal for MOSFET Q2. Input voltage, output voltage and gate signal of SBC.

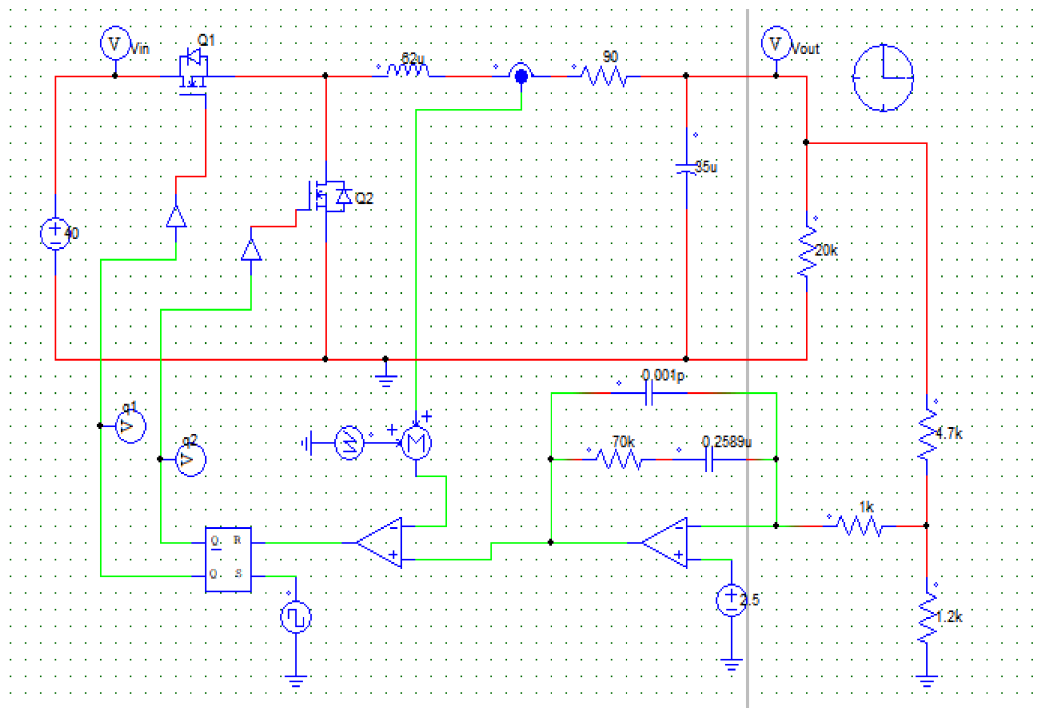


Figure 8. Simulation circuit of SBC by using CMC.

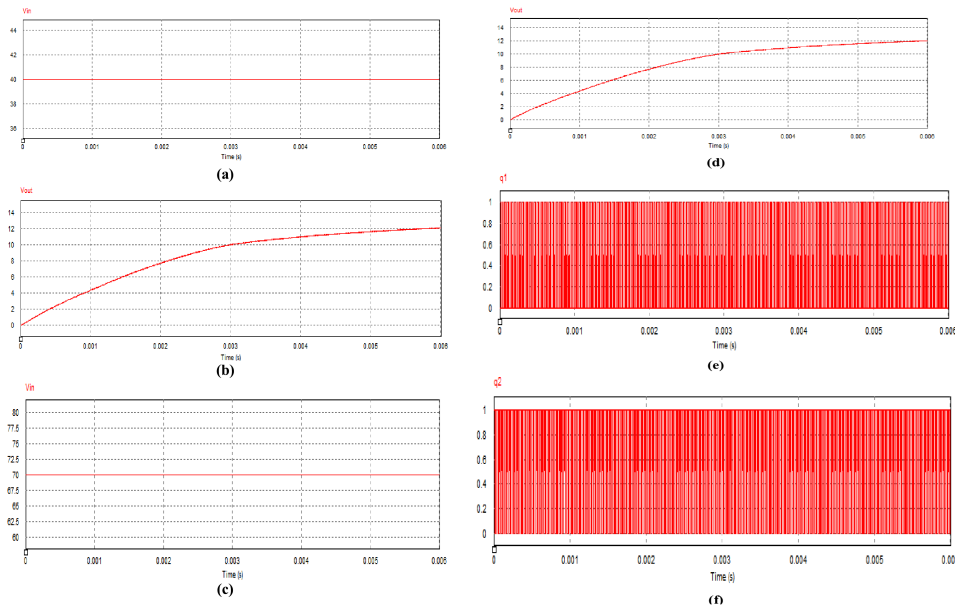


Figure 9. (a) Input voltage waveform of 40 V. (b) Output voltage waveform of 12 V for 40 V input. (c) Input voltage waveform of 70 V. (d) Output voltage waveform of 12 V for the 70 V input. (e) Gate signal for MOSFET Q1. (f) Gate signal for MOSFET Q2.

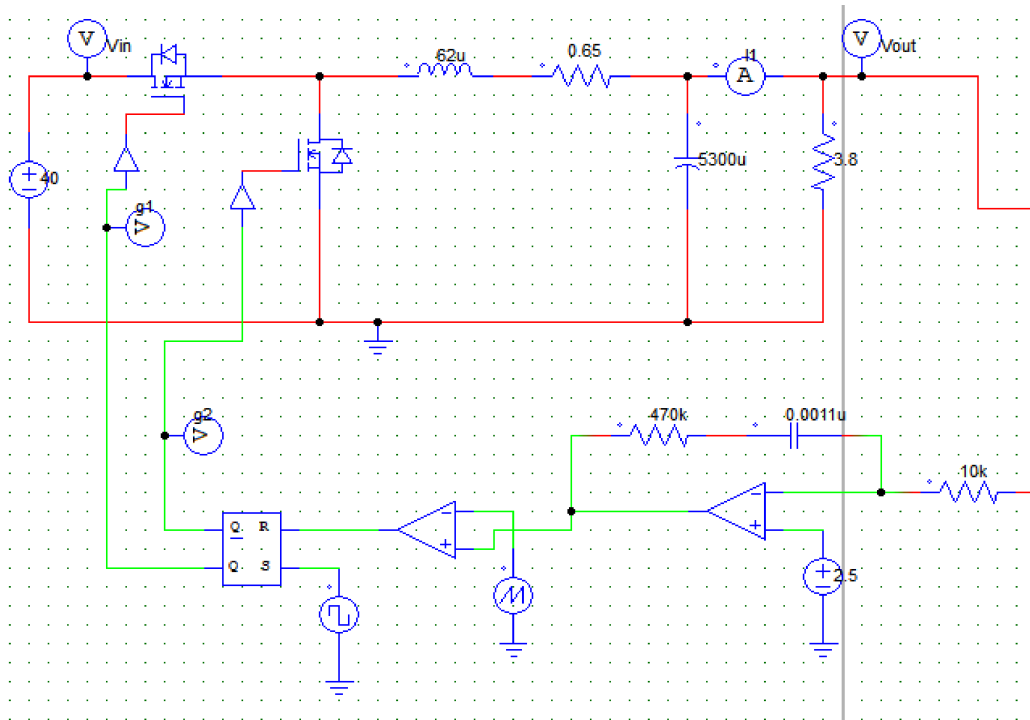


Figure 10. Simulation of SBC by using VMC.

6. Hardware implementation

SBC which consists of two MOSFET (one act has low side, MOSFET and the other act as high side MOSFET) is implemented in hardware. The designed SBC is tested under no load condition.

Wide range input SBC is implemented by using emulated peak current mode control method. The synchronous buck converter lowers power losses compared to a traditional

buck converter by swapping a power MOSFET for the commutating diode. Voltage drop across the diode can be reduced by using MOSFET. The internal resistance of MOSFET is less hence the drop across the MOSFET is less than that of drop across the diode in ABC.

Wide range input voltage of SBC is shown in Fig. 12. The output voltage is regulated if the input voltage is varied from 40 V to 75 V. The switching frequency is 50 kHz.

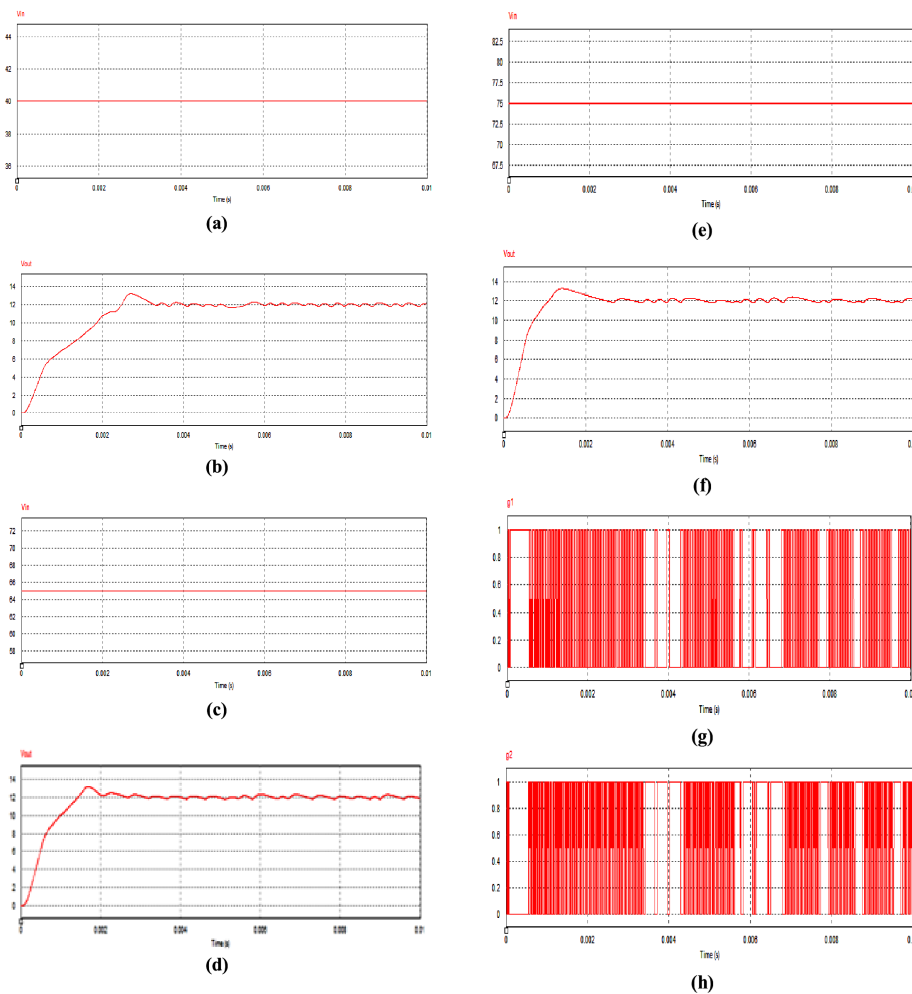


Figure 11. (a) Waveform of input voltage for 40 V. (b) Output voltage waveform of 12V for 40 V input. (c) Wave form the SBC for 65 V input. (d) Output voltage waveform for 65 V input. (e) Waveform of SBC for 75 V input. (f) Output voltage waveform of SBC for 75 V input. (g) Gate signal for MOSFET Q1. (h) Gate signal for MOSFET Q2.



Figure 12. Prototype of Wide range input SBC.

From the above test it is noted that for the respective input voltage the regulated output voltage is obtained for varying current rating of load. Load test for the currents of 1 A, 2 A, 3 A, 4 A and 5 A of SBC are conducted and the respective

Input and output voltages are illustrated in Table 3 to Table 7 respectively.

Table 3. Load test of SBC for 1 A.

Input voltage (V)	Output voltage (V)
45	12.39
50	12.38
55	12.38
60	12.38
65	12.38

Table 4. Load test of SBC for 2 A.

Input voltage (V)	Output voltage (V)
45	12.36
50	12.36
55	12.36
60	12.36
65	12.36

Table 5. Load test of SBC for 3 A.

Input voltage (V)	Output voltage (V)
45	12.34
50	12.34
55	12.34
60	12.34
65	12.34

Table 6. Load test of SBC for 4 A.

Input voltage (V)	Output voltage (V)
45	12.32
50	12.32
55	12.32
60	12.32
65	12.32

Table 7. Load test of SBC for 5 A.

Input voltage (V)	Output voltage (V)
45	12.30
50	12.30
55	12.30
60	12.30
65	12.30

7. Conclusion

A wide range input SBC is designed for EV application with input voltage range of 40 – 75 V and output voltage of 12 V. The converter has been simulated and tested in three modes of operation namely, i) Emulated Peak Current Mode ii) Current Mode Control, and iii) Voltage Mode

Control. Wide range converter is implemented and the detailed loss calculation analysis of SBC is made and it was found that SBC has its losses reduced by 8%. The replacement of MOSFET (any controlled switches) in the place of diode leads to less losses in the proposed SBC. Thus, the SBC using EPCM, CMC and VMC is simulated by using PSIM and the results are presented. The hardware set up of the converter with EPCM has been tested and the results are tabulated. Variations in the waveform for various control technique is observed. SBC was practically tested under load conditions for different current ratings. The output voltage is very well regulated when the input voltage is in the range of 40 V to 75 V for various load conditions in the implemented converter system.

Authors contributions

All authors have contributed equally to prepare the paper.

Availability of data and materials

The data that support the findings of this study are available from the corresponding author upon reasonable request.

Conflict of interests

The authors declare that they have no known competing financial interests or personal relationships that could have appeared to influence the work reported in this paper.

Open access

This article is licensed under a Creative Commons Attribution 4.0 International License, which permits use, sharing, adaptation, distribution and reproduction in any medium or format, as long as you give appropriate credit to the original author(s) and the source, provide a link to the Creative Commons license, and indicate if changes were made. The images or other third party material in this article are included in the article's Creative Commons license, unless indicated otherwise in a credit line to the material. If material is not included in the article's Creative Commons license and your intended use is not permitted by statutory regulation or exceeds the permitted use, you will need to obtain permission directly from the OICC Press publisher. To view a copy of this license, visit <https://creativecommons.org/licenses/by/4.0>.

References

- [1] P. Sweety, P. Subha Hency, G. Wessley, and P. Rajalakshmy. "Environmental impact of electric vehicles.". *E-Mobility*, page pp. 31–42, 2021. DOI: https://doi.org/10.1007/978-3-030-85424-9_2.
- [2] I. Azizi and H. Radjeai. "A bidirectional dc-dc converter fed dc motor for electric vehicle

- application.**”. *2015 4th International Conference on Electrical Engineering (ICEE)*, 2015. DOI: <https://doi.org/10.1109/intee.2015.7416683>.
- [3] G. Chen, Y. Deng, J. Dong, Y. Hu, L. Jiang, and X. He. “**Integrated multiple-output synchronous buck converter for electric vehicle power supply.**”. *IEEE Transactions on Vehicular Technology*, 66(7):pp. 5752–5761, 2017. DOI: <https://doi.org/10.1109/tvt.2016.2633068>.
- [4] D. L. Del Moral, A. Barrado, M. Sanz, P. Zumel, C. Raga, A. Lazaro, and H. Miniguano. “**Improvement of the synchronous buck converter dynamic performance applied to hybrid electric vehicle regenerative power systems.**”. *2015 9th International Conference on Compatibility and Power Electronics (CPE)*, 2015.
- [5] M. R. Uddin, Z. Tasneem, S. I. Annie, and K. M. Salim. “**A high capacity synchronous buck converter for highly efficient and lightweight charger of electric easy bikes.**”. *2017 International Conference on Electrical, Computer and Communication Engineering (ECCE)*, 2017. DOI: <https://doi.org/10.1109/ecace.2017.7912936>.
- [6] K. I. Hwu, J. J. Shieh, and W. Z. Jiang. “**Analysis and design of type 3 compensator for the buck converter based on psim.**”. *13th IEEE Conference on Industrial Electronics and Applications (ICIEA)*, 2018. DOI: <https://doi.org/10.1109/iciea.2018.8397859>.
- [7] O. Hegazy, J. Van Mierlo, and P. Lataire. “**Design and control of bidirectional dc/ac and dc/dc converters for plug-in hybrid electric vehicles.**”. *International Conference on Power Engineering, Energy and Electrical Drives*, 2011. DOI: <https://doi.org/10.1109/powereng.2011.6036530>.
- [8] P. Sweety, M. Geetha, J. Kanakaraj, and C. Abinaya. “**Power quality improvement by direct power control of active front end rectifier.**”. *Journal of Scientific and Industrial Research (JSIR)*, 76(6):pp. 339–342, 2017.
- [9] S. Farhani and F. Bacha. “**Modeling and control of a dc-dc resonant converter interfacing fuel cell in electric vehicle.**”. *9th International Renewable Energy Congress (IREC)*, 2018. DOI: <https://doi.org/10.1109/irec.2018.8362507>.
- [10] P. Sweety and M. Muthulakshmi. “**Vienna rectifier for electric vehicle charging station.**”. *International Journal of Mechanical Engineering*, 6(3):pp. 511–516, 2021.
- [11] S. Cui, D. He, Z. Chen, and T. G. Habetler. “**A wide input voltage range zvs isolated bidirectional dc-dc converter for ultra-capacitor application in hybrid and electric vehicles.**”. *IEEE International Electric Vehicle Conference*, 2012. DOI: <https://doi.org/10.1109/ievc.2012.6183239>.
- [12] A. K. Singha, S. Kapat, and J. Pal. “**A robust design framework for stable digital peak current-mode control under uniform sampling.**”. *IEEE Energy Conversion Congress and Exposition (ECCE)*, 2016. DOI: <https://doi.org/10.1109/ecce.2016.7854769>.
- [13] W. Z. Jiang, J. S. Lai, and K. I. Hwu. “**Digital compensator design for high-frequency hybrid resonant buck converter.**”. *7th International Symposium on Next Generation Electronics (ISNE)*, 2018. DOI: <https://doi.org/10.1109/isne.2018.8394706>.
- [14] J. M. Choi, B. J. Byen, Y. J. Lee, D. H. Han, H. S. Kho, and G. H. Choe. “**Design of leakage inductance in resonant dc-dc converter for electric vehicle charger.**”. *IEEE Transactions on Magnetics*, 48(11):pp. 4417–4420, 2012. DOI: <https://doi.org/10.1109/tmag.2012.2196027>.
- [15] M. Santhi, R. Rajaram, and I. G. C. Raj. “**Converter circuit for battery-fuel cell hybrid systems.**”. *IEEE Conference on Electric and Hybrid Vehicles*, 2006. URL [10.1109/icehv.2006.352288](https://doi.org/10.1109/icehv.2006.352288).